Proceedings Paper:
Abrams, K.J., Wan, Q., Stehling, N. et al. (2017) Nanoscale mapping of semi-crystalline polypropylene. In: Physica Status Solidi (C). European Materials Research Society Spring 2017, 22-26 May 2017, Strasbourg, France. Wiley. ISSN: 1862-6351. EISSN: 1610-1634.

https://doi.org/10.1002/pssc.201700153

pss-Header will be provided by the publisher

Nanoscale mapping of semi-crystalline polypropylene

Kerry J. Abrams [*,1], Quan Wan[1], Nicola A Stehling[1], C.Jiao[2], A.C. S Talari[1], Ihtesham Rehman[1] and Cornelia Rodenburg [,1]**

[1]Department of Material Science and Engineering, University of Sheffield, Sheffield, S10 2TN, UK.

[2]Thermo Fisher Scientific, Materials & Structural Analysis (formerly FEI), Achtseweg Noord 5, 5651 GG Eindhoven, the Netherlands

Received ZZZ, revised ZZZ, accepted ZZZ
Published online ZZZ (Dates will be provided by the publisher.)

Keywords Secondary electron spectroscopy, semi-crystalline polymers, hyperspectral imaging, polypropylene.

We reveal nanoscale information of semi-crystalline polypropylene with the use of a new secondary electron hyperspectral imaging technique. The innovative combination of cryo-SEM and low voltage allows for the optimised imaging of these beam-sensitive materials. Through the collection of secondary electron hyperspectral imaging data mapping of molecular order on the nanoscale in the scanning electron microscope (SEM) can be achieved.

1 Introduction **Understanding the structure-property relationship of semi-crystalline polymers is essential for the optimisation for next generation materials. Their hierarchical nature means the macro- and micro- properties correlate down through the length scales from micrometres to nanometres [1]. Typically, multiple techniques are used to probe these materials such as scanning electron microscopy (SEM), atomic force/scanning probe microscopy and X-ray diffraction [1]. From these, scanning electron microscopy is contact-free and has a great potential for insights into a polymers' nano-morphology since high resolution images can be obtained over a large horizontal field of view (>10s µm) and, further, via the use of low accelerating voltages, beam damage is reduced and the need for conductive coating [2, 3] eliminated. Secondary Electron (SE) Spectroscopy has previously been carried out on carbon fibres [4] and changes in the SE spectrum were linked to nano-scale structural differences. Furthermore, SE spectroscopy in the SEM has been previously used to map dopants in semiconductors [5] and phases in organic photovoltaics [6,7]. Here we apply to microporous polypropylene and additionally, map the conformational order. Microporous polypropylene is a heterogeneous semi-crystalline polymer which can be described as a three phase composite. The phases differ only in conformation, ranging from ordered crystalline (close packed long chain helices) to an amorphous (randomly coiled helices or very short chain helices) with an intermediate phase often termed mesophase (an ordered state of the amorphous region) [8,9]. The ratio of these phases will depend on the crystallization conditions, processing parameters and thermal history [8]. Furthermore, the end point strength, and ultimate function of the polymer will depend significantly on the interplay of these phases e.g. it is the different response to shear forces of each phase that leads to polypropylene being one of the most common polymers used to form porous films. These membranes hold interest for use in many industrial applications including quantum dot templates [10], antifouling films [11] and battery separators in Li-ion batteries [12]. In this work, we carry out low energy SEM and Raman hyperspectral imaging to elucidate on the micron scale and then secondary electron hyperspectral imaging (SEHI) to maximise contrasts from the different phases in microporous polypropylene, to enable mapping on the nanoscale of semi-crystalline polypropylene.**

* Corresponding author: Kerry.Abrams@sheffield.ac.uk , Phone: +44 222 5989, Fax: +00 999 999 999
** e-mail Cornelia.Rodenburg@sheffield.ac.uk , Phone: +44 222 5921, Fax: +00 999 999 999

2 Experimental

2.1 Preparation of semi-crystalline microporous polypropylene. For morphological analysis on the micron scale, the microporous polypropylene 20 μm thick films with 40 % volume (films obtained from Innovia films Ltd) were cut into 5 mm squares and characterised by Raman spectroscopy. A DXR Raman Microscope (Thermo- Scientific) was utilised with a laser wavelength of 532 nm over a spectral range of (3200–600) cm-1. To ensure that Raman information was indicative of the film (i.e. covered the porous and the crystalline regions) both point spectra and 50 micrometre line maps were recorded.

For morphological analysis at the nanoscale, plan view samples were contacted to a SEM stub. Cross-section samples were cut down to size, sandwiched between silicon wafers with Scigen OCT compound and plunged into liquid nitrogen before transferring into the SEM via a cryo-preparation chamber. The microporous polypropylene sandwich was cryo-fractured in-situ and subjected to a sublimation for 5 minutes at 70 °C to remove any residual ice on the cleaved surface. No conductive coating was added.

2.2 Low Voltage Secondary Electron Imaging and Secondary Electron Hyperspectral Imaging For analysis at the micrometre scale , a Helios Nanolab G3 UC Scanning Electron Microscope (SEM) in Cryo mode was used in secondary electron (SE) imaging mode and the Everhart-Thornley Detector was selected. This SEM is specifically designed for high resolution imaging at low voltages (<1kV.) An accelerating voltage of 500V and a working distance of 4 mm was used

For film analysis at the nanoscale, SE hyperspectral imaging (SEHI) was carried out in Cryo-mode. For this technique, the in-lens detector was selected. The design of this detector allows for the different SE energy ranges to be collected by changing a mirror voltage [13,14]. An iFast automatic collection recipe (iFast developers kit version 3.0.16.1738) was utilised to step the mirror voltage between -15V and 15V and an image was collected with each successive 0.5V. The mean intensity of each micrograph was plotted for each mirror voltage and the final SE spectra were generated by differentiating the intensity of the micrographs with respect to the mirror voltage step. The resulting SE spectra are characteristic of the surface of the material. Further high resolution images were recorded at the specific mirror voltage settings associated with features of interest on the films. All images were processed in Image J (version 1.51j).

3 Results and discussion

3.1 Semi-crystalline polypropylene features on the micron scale Crystallinity investigations on the micrometre scale of polypropylene is well established using Raman spectroscopy [15,16]. The Raman bands of 809cm^{-1} and 841 cm^{-1} are said to be spectral markers of crystallinity, that is, as the crystallinity increases the intensity of the 809 cm^{-1} peak increases with respect to the 841 cm^{-1} peak. Furthermore, Nielsen et al concluded that the 809 cm^{-1} band corresponds to the longer helical chains associated with the 3D architecture and the 841 cm^{-1} band is a result of shorter helical chains associated with the amorphous or mesophase regions [17]. A typical Raman spectrum of microporous polypropylene is shown in Figure 1a) with insert 1e) showing an enlargement of the 809 cm^{-1} and 841 cm^{-1} peaks. The hyperspectral plots 1b) and 1c) show the average intensity changes for these two wavenumbers over an area of of 50 by 25 microns. It is quite clear that the average level of crystallinity (the ratio of 809 cm^{-1} to 841 cm^{-1}) changes considerably over this distance and the values of these two peaks are closely related. These maps reveal neighbouring areas of high crystallinity and low crystallinity on the micron scale.

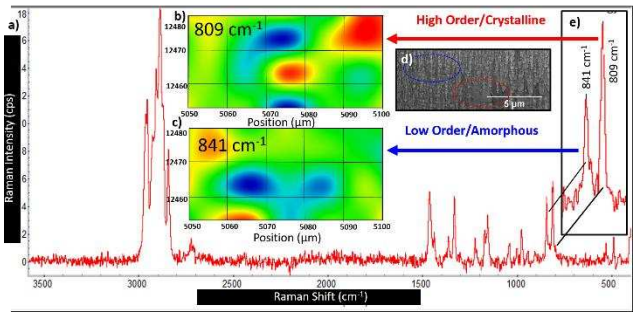

Figure 1 a) A Raman spectrum from 300-3200 cm-1 showing Raman peaks in MPP, b) Hyperspectral map of 809 cm-1, c) hyperspectral map of 841 cm-11, d) SEM micrograph showing amorphous and crystalline regions e) Enlarged inset of 809 cm-1 and 841 cm-1

To elucidate the relationship between the variation in Raman signal due to crystallinity differences and the morphological features in the films on smaller length scales, we utilise low voltage SEM. Figure 2 a) is a standard micrograph which covers the typical field of view as the Raman map in Figure 1c). At this length scale, flaws and defects can be observed on the film, however, the contrast is relatively uniform with a slight topographical contrast. The fabrication of microporous polypropylene is achieved by the annealing of a precursor film which has previously been uniaxially stretched to produce a row-nucleated lamellar crystalline

structure and then further stretched [18]. The anneal step results in the crystalline lamellae surrounded by amorphous regions becoming thicker and more stable by the reordering of the polymer chains along the amorphous/crystalline interface and the formation of metastable crystalline zones (sometimes referred to as daughter crystals.) The subsequent stretch acts to form pores by disentangling the amorphous chains to form bridges between the lamellae and also causes the reorientation of the daughter crystals inside the lamella (For appropriate schematics, the reader is guided to literature [18,19].

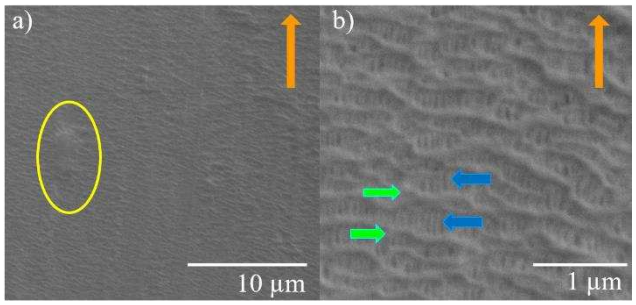

Figure 2 a) Low magnification standard SE micrograph of microporous polypropylene showing typical morphology, flaws are highlighted by the yellow circle. This magnification is on the scale of the Raman map ns in Figure 1b) and c), b) A higher magnification standard SE micrograph revealing lamellae (green arrows) and region containing pores (blue arrows); Both a) and b) were taken using Everhart-Thornley detector. All images were taken in plan view using 500V and working distance of 4 mm. Orange arrow highlights the extrusion direction (ED).

The low voltage analysis allows us to obtain higher magnification, Figure 2b, shows the typical morphology i.e. lamella (highlighted by the green arrows) interlaced with porous regions (highlighted by the blue arrows). The highly crystalline lamellae are connected by bridges that separate pores which are elongated in the direction of film extrusion, (highlighted by the orange arrow). The average pore length is 150 nm. According the published models for pore formation in polypropylene [18, 20- 22], the material surrounding the pores (bridges) is more disordered than the lamella. So as our materials are porous, they will essentially be composed of two phases-crystalline and oriented amorphous. But this ordinary SEM imaging mode shows little variance in the contrast between these phases.

3.2 Semi-crystalline polypropylene features on the nano- scale

If we apply our SEHI technique to our microporous polypropylene film, that is, control which SE energy is allowed to reach the detector, finer contrast differences can be observed. Figure 3a) shows a SE spectra obtained from a cross-sectional sample The SE spectra shows a characteristic shape for microporous polypropylene and the dominant peak is around the central mirror voltage setting. The micrograph in figure 3b) is unfiltered so contains all the SE energies from all the mirror voltage settings. In this cross-sectional orientation, the crystalline and pores layers are not so parallel (most likely to be caused by smearing from the cryo-fracture procedure) but they can quite clearly be observed (highlighted by the blue and green arrows). There are now different contrasts associated with different regions of the film with the crystalline lamellae, the pore bridges and the pores. Some literature describes the oriented amorphous bridges as fibrils [20]. The average fibril width is 25 nm. One can observe that these fibrils connect through to different pore layers as per the expected pore formation models [18, 20-22].

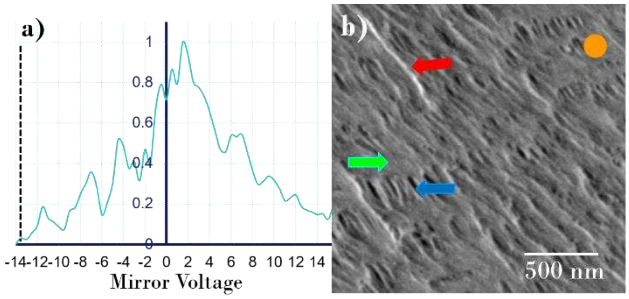

Figure 3 a) Cross-sectional SE spectra of microporous polypropylene showing characteristic peaks b) Associated SEHI taken with the in-lens detector formed from all secondary electron energies. Acceleration voltage 500V, in lens detector and working distance of 4 mm. Green arrows highlight lamella, blue arrows highlight pores, red arrow highlights a fibril and the orange circle shows extrusion direction which is now into the film.

3.3 Nanoscale Mapping

As previously stated, it has been shown that isolation of certain spectral features by imaging with just those mirror voltages associated allows the selection of those contributions and filters out the other energies. Figure 4a) once again shows the spectrum of microporous polypropylene and the associated images recorded with only the mirror voltages highlighted by the green, orange and purple dashed lines. Figure 4b) shows the mirror voltage selection from the green and orange dashed lines and an increase in contrast for the oriented amorphous bridges is observed. With an increase in contrast in the crystalline lamella regions observed from the isolation of the major peak in the spectra (between the orange and purple lines) Figure 4c). Additionally, the average nano-crystallites size can now be analysed and is less than 50 nm. Figure 4d) shows the image from the mirror voltage setting highlighted by the

purple line, this images loses all aforementioned contrast. Microporous polypropylene is elementally uniform therefore the differences in electron emission must be associated with the conformational order within this material. This image series (from minimum to maximum mirror voltage) clearly shows that the isolation of peaks within this SE spectrum can enhance the resolution of that region by filtering out energies that do not originate from that feature. In short, SEHI allows the imaging of this semi-crystalline polypropylene at the nanoscale.

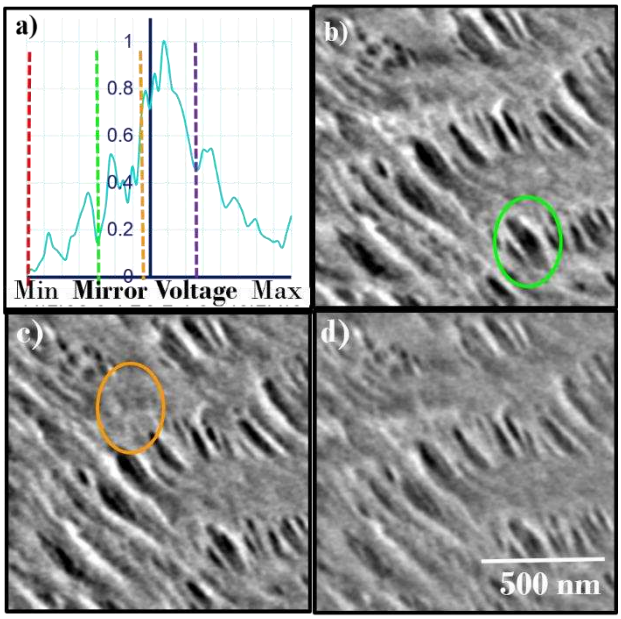

Figure 4 a) SE spectrum of microporous polypropylene with specific mirror voltage settings highlighted by the coloured dashed lines b) SEHI micrograph recorded using the mirror voltages between the green and orange line, the green circle highlights optimised contrast for the oriented amorphous phase c) SEHI micrograph recorded using the mirror voltages between the orange and purple lines, the orange circle exhibits optimised contrast for the crystalline lamella d) SEHI micrograph recorded using the mirror voltages above the purple line. All images taken with acceleration voltage 500V, in lens detector and working distance of 4 mm.

4 Conclusion Here we demonstrate hyperspectral imaging based on secondary electron signals in the scanning electron microscope as a means to map molecular order on different length scales (nano- to tens of microns) in microporous polypropylene. This type of SE spectroscopy in the SEM at low voltages at cryo-temperatures hold significant potential to providing fundamental insights into the nano-morphology of beam-sensitive synthetic polymers. Future work lies in the understanding morphological changes caused by plasma treatment and correlation with their intrinsic mechanical properties.

Acknowledgements Kerry Abrams would like to thank the Sorby Centre for Microscopy and Microanalysis for the access to the electron microscope and related equipment. Cornelia Rodenburg and Kerry Abrams are grateful to EPSRC for support under EP/N008065/1. All authors are grateful to our Collaborators: M. Uncovsky and T. Vystavel (Thermo Fisher Scientific, Materials & Structural Analysis (formerly FEI), Vlastimila Pecha 1282/12, 627 00 Brno, Czech Republic) for their expertise and support and Innovia Films, J. Moffat and C. Holliday, for sample materials and expertise (Innovia Films Ltd, Lowther R&D Centre, West Road, Wigton, Cumbria, CA7 9XX, UK.)

References

[1] Michler, G H. Electron Microscopy of Polymers, (2008 Springer-Verlag Berlin Heidelberg.)
[2] Reimer, L. Image formation in Low-Voltage Scanning Electron Microscopy (1993 SPIE Optical Engineering Press.)
[3] Joy D. Low Voltage SEM. J. Microsc. 140, 282 (1985.)
[4] Willis, R.F., Feuerbacher, B. and Fitton, B, Physics Lett. 34A (1971).5] Rodenburg C., Jepson, M.A.E., Bosch, E.G.T and Dapor, M. Ultramicroscopy, 110, 1185-1191(2010).
[6] Masters, R. C., Pearson, A.J., Glen, T.S. Sasam, F-C, Li, L., Dapor M., Donald, A.M., Lidzey, D.G and Rodenburg, C., Nature Commun., 6, 6928 (2015).
[7] Kumar, V., Schmidt, W.L., Schileo,G., Masters, R.C., Wong-Stringer, M., Sinclair, D.C., Reaney, I.M., Lidzey, D and Rodenburg, C., ACS Omega, 2, 2126 (2017)
[8] Lotz B.; Fillon B.; Thierry A.; Wittmann J-C. , Polymer. Bull., 25, 101-105 (1991.)
[9] Androsch R.; Lorenzo D. M.; Schick C.; Wunderlich B, Polymer, 51, 4639 (2010.)
[10] Bobrovsky A., Shibaev, V., Abramchuk,S., Slyshevitch,G., Samokhvalov,P., Oleinkov,V. and Mochalov,K., European Polymer Journal, 82, 93-101(2016.)
[11] Lin Y., Meng, L., Wu, L., Li, X., Chen, X., Zhang, Q, Zhang,R., Zhang, W. and Li, L, Polymer, 80, 214 (2015)
[12] Yang Y-F., Wan, L-S and Xu, Z-K., , Journal of Adhesion Science and Technology,25, 1539-1548 (2011.)
[13] Kazemian, P. Mentink, S.A.M., Rodenburg, C. and Humphreys, C.J. , Ultramicroscopy,107, 140 (2007.)
[14] Young, R. Bosch, E, Uncovsky, M. and Tuma, L. , Microscopy Microanalysis, 15, 222 (2009.)
[15] Arruebarrena de Baez, M., Hendra, P.J, and Judkins, M. , Spectrochimica Acta A, 51, 2117-2124 (1995.)
[16] Paradkar R. P.; Patel R. M.; Knickerbocker E. and Doufas A. J. Applied Polymer Science 109, 3413-3420 (2008.)
[17] Nielson A. S.; Batchelder D. N.; Pyrz R, Polymer, 43, 2671-2676 (2002.)
[18] Chen X., Xu, R., Xie,J. Lin, Y, Lei, C. and Li. L. , Polymer, 94, 31-42 (2016.)
[19] Qiu J., Wang, Z., Yang, L. Zhao, J. Niu,Y. and Hsiao, B.S., Polymer, 48, 6934-6947 (2007.)
[20] Xu R. J.; Lei C.; Cai Q.; Hu B.; Shi W.; Mo H.; Chen C , Plastic Rubber Composites, 43, 257-263 (2014.)
[21] Saffar A.; Ajji A.; Carreau P. J.; Kamal M. R., Polymer, 55, 3156-3167 (2014.)
[22] Tabatabaei S. H.; Carreau P. J.; Ajji A, Polymer, 50, 3981-3989 (2009.)